Tellus (2002), 54B, 325–343
Printed in UK. All rights reserved

TELLUS
ISSN 0280–6509

Long-term evolution of the global carbon cycle: historic minimum of global surface temperature at present

By SIEGFRIED FRANCK[1]*, KONRAD J. KOSSACKI[2], WERNER VON BLOH[1] and CHRISTINE BOUNAMA[1], [1]*Potsdam Institute for Climate Impact Research, PF 601203, 14412 Potsdam, Germany;* [2]*Institute of Geophysics of Warsaw University, Pasteura 7, 02-093 Warsaw, Poland*

(Manuscript received 21 August 2001; in final form 30 May 2002)

ABSTRACT

We present a minimal model for the global carbon cycle of the Earth containing the reservoirs mantle, ocean floor, continental crust, continental biosphere, and the kerogen, as well as the aggregated reservoir ocean and atmosphere. This model is coupled to a parameterised mantle convection model for describing the thermal and degassing history of the Earth. In this study the evolution of the mean global surface temperature, the biomass, and reservoir sizes over the whole history and future of the Earth under a maturing Sun is investigated. We obtain reasonable values for the present distribution of carbon in the surface reservoirs of the Earth and find that the parameterisation of the hydrothermal flux and the evolution of the ocean pH in the past has a strong influence on the atmospheric carbon reservoir and surface temperature. The different parameterisations give a rather hot as well as a freezing climate on the early Earth (Hadean and early Archaean). Nevertheless, we find a pronounced global minimum of mean surface temperature at the present state at 4.6 Gyr. In the long-term future the external forcing by increasing insolation dominates and the biosphere extincts in about 1.2 Ga. Our study has the implication that the Earth system is just before the point of evolution where this external forcing takes over the main influence from geodynamic effects acting in the past.

1. Introduction

On geological time scales, the Earth's climate is believed to be mainly determined by atmospheric CO_2 variations. There have been a number of studies (e.g., Walker, 1977; Holland, 1978; 1984; Franck et al., 1999) investigating the global carbon cycle between mantle and surface reservoirs to regulate atmospheric CO_2 levels against increasing insolation. Nevertheless, nobody knows whether the so-called Hadean era at the beginning of Earth's history was really a greenhouse era with surface temperatures up to 80 °C (Kasting and Ackermann, 1986; Schwartzman, 1999), or an ice-house (Sleep and Zahnle, 2001). Although CO_2 alone could, in principle, solve the faint young Sun problem, there are some grounds for suspecting other greenhouse gases to be involved. Mineralogical investigations of ancient soils by Rye et al. (1995) seem to set an upper limit of about 30 present atmospheric CO_2 levels on p_{CO_2} in the Archaean, insufficient to prevent freezing unless there are other greenhouse gases. A favoured reduced gas has been CH_4, which is consistent with low O_2 levels before 2.0–2.2 Ga (Walker et al., 1983; Kasting, 1993; Pavlov et al., 2000; Kasting et al., 2001).

In the present paper we investigate a minimal model for the global carbon cycle between the mantle and five surface reservoirs: ocean floor, continental crust, continental biosphere, ocean + atmosphere, and the kerogen, i.e., dispersed insoluble organic carbon in rocks. Kerogen results from a very small portion of organic carbon that is not transformed back to CO_2 by respiration and decay, but is accumulated to a remarkable reservoir. The reservoir size of carbon in

*Corresponding author.
e-mail: franck@pik-potsdam.de

the present living biosphere is even smaller than the amount of carbon in the present atmosphere. Nevertheless, the biosphere plays a main role in the controlling process of the terrestrial climate and is necessary for kerogen accumulation. From the point of view of carbon cycling, kerogen could be important, even if it is relatively inert, and can be only brought back into the carbon cycle by oxidation with the help of atmospheric O_2 or bacteria. It occupies about 10–20% (Holland, 1978; Kasting and Walker, 1992) of the total present amount of carbon in the surface reservoirs and therefore has to be included in a minimal model.

There are also much more sophisticated models for the circulation of carbon only among the surface reservoirs. In such models the subducting seafloor carbonates are metamorphosed completely and all the CO_2 returns to the atmosphere through arc volcanism without any mantle regassing. Furthermore, there is no mantle degassing at mid-ocean ridges. This cycle is known as the "Carbonate–Silicate Geochemical Cycle" (see, e.g. Walker et al., 1981; Berner et al., 1983; Lasaga et al., 1985). The "Global Carbon Cycle" is related to time scales longer than 10^5 a (Kasting, 1984; Volk, 1987). At shorter time scales various processes involved have to be described in much more detail, as is done for example in the GEOCARB II/III model of Berner (1994) and Berner and Kothavala (2001).

Special attention in our carbon cycle modelling is given to the hydrothermal carbonatisation, i.e. the reaction of circulating hydrothermal seawater with basalts from mid-ocean ridges to form carbonates. For the parameterisation of the hydrothermal flux we use three different approximations: at first the hydrothermal flux is fixed over time to the present day value, next it is proportional to production of fresh basalt at mid-ocean ridges (slow reaction kinetics), and finally we follow Sleep and Zahnle (2001) in assuming fast reaction kinetics with a superabundance of cations. Fast reaction kinetics may produce rather low levels of atmospheric CO_2 in the early Earth. A similar effect may result from the reaction of CO_2 with Hadean impact ejecta and its subduction (Sleep and Zahnle, 2001). However, we will not consider such effects because the influence of impacts on the volatile inventory remains a subject of discussion (Bounama et al., 2001).

Another important point in our carbon cycle modelling is the oceanic pH, which controls the partitioning of CO_2 between the ocean and the atmosphere. Up to now there is no definitive agreement about the oceanic pH in the past: Grotzinger and Kasting (1993) give arguments for a relative constancy of pH, Kempe and Kazmierczak (1994) favour a so-called soda ocean, and Macleod et al. (1994) and Russell and Hall (1997) conclude that the early ocean was acid. According to Walker (1985) an oceanic pH lower than 6.5 implies that more CO_2 is in the atmosphere than in the ocean. In our modelling scheme we investigate the following scenarios: constant oceanic pH, a linear increase of oceanic pH (acid ocean in the past), and a linear decrease of oceanic pH (soda ocean in the past).

In general, the chemistry of the ocean is dominated by two principal fluxes: the "river flux" from weathering of the continents and the "mantle flux" from the mid-oceanic ridges (Godderis and Veizer, 2000). Both effects are incorporated in our model. Silicate weathering rates are proportional to the continental area, because for long time scales the silicate reservoir is proportional to the continental surface area in a first approximation. On shorter time scales, effects of fresh rock production by continental uplift (Ruddiman, 1998) or by impacts (Koster van Groos, 1988) may temporarily increase weathering processes. The dependence of the hydrothermal flux on the spreading rate will be discussed in detail in the present paper.

The dynamical character of the model means that the effective carbon flux to or from each of the reservoirs is integrated over time. In this way, the present state of the Earth system is not the starting point for the modelling, as in our previous work (Franck et al., 1999, 2000a,b), but the result of the Earth's evolution over 4.6 Ga. On the other hand, within the new procedure we need some initial conditions that are only poorly constrained. Our formalism is a modified and extended version of that described by Tajika and Matsui (1990, 1992) and Sleep and Zahnle (2001). We use a significantly improved algorithm and account for two more carbon reservoirs (continental biosphere and kerogen). The global carbon cycle model is coupled to the thermal and degassing history of the Earth with the help of a parameterised model of mantle convection with volatile exchange (Franck and Bounama, 1995; Franck et al., 2000a).

The main focus of our investigations is the analysis of the self-regulation via feedback loops that respond to external forcings on the ecosphere. It is evident that the interactions within the Earth system, and therefore also the self-regulation, will change in many ways in Earth's history. So we come to the questions, how did the Earth system operate in the past, how does it operate at present, and how will it operate in the long-term

future? To answer these, it is necessary to investigate different scenarios for the past and future evolution of the various carbon pools and the global mean surface temperature.

2. Model description

The model describes the evolution of the mass of carbon in the mantle, C_m, in the ocean crust and floor, C_f, in the continental crust, C_c, in the continental biosphere, C_{bio}, in the kerogen, C_{ker}, and in the combined reservoir consisting of ocean and atmosphere, C_{o+a}. The equations for the efficiency of carbon transport between reservoirs take into account degassing and regassing of the mantle, carbonate precipitation, carbonate accretion, evolution of continental biomass, the storage of dead organic matter, and weathering processes. Thus, the basic equations are:

$$\frac{\mathrm{d}C_m}{\mathrm{d}t} = \tau_f^{-1}(1-A)RC_f - S_A f_c d_m C_m / V_m \tag{1}$$

$$\begin{aligned}\frac{\mathrm{d}C_{o+a}}{\mathrm{d}t} &= \tau_f^{-1}(1-A)(1-R)C_f + S_A f_c d_m C_m / V_m \\ &\quad + F_{\text{weath}} + (1-\gamma)\tau_{\text{bio}}^{-1} C_{\text{bio}} + \tau_{\text{ker}}^{-1} C_{\text{ker}} \\ &\quad - \Pi_{\text{bio}} - F_{\text{prec}} - F_{\text{hyd}}\end{aligned} \tag{2}$$

$$\frac{\mathrm{d}C_c}{\mathrm{d}t} = \tau_f^{-1} A C_f - F_{\text{weath}} \tag{3}$$

$$\frac{\mathrm{d}C_f}{\mathrm{d}t} = F_{\text{prec}} + F_{\text{hyd}} - \tau_f^{-1} C_f \tag{4}$$

$$\frac{\mathrm{d}C_{\text{bio}}}{\mathrm{d}t} = \Pi_{\text{bio}} - \tau_{\text{bio}}^{-1} C_{\text{bio}} \tag{5}$$

$$\frac{\mathrm{d}C_{\text{ker}}}{\mathrm{d}t} = \gamma \tau_{\text{bio}}^{-1} C_{\text{bio}} - \tau_{\text{ker}}^{-1} C_{\text{ker}}. \tag{6}$$

The variable t is the time, S_A the areal spreading rate, A the accretion ratio of carbon ($A > 0$ for $A_o < A_e$), A_e the area of the Earth, A_o the area of the ocean basins, R the regassing ratio, f_c the degassing fraction of carbon, d_m the melt generation depth parameterised according to McKenzie and Bickle (1988), V_m the mantle volume, F_{weath} the weathering rate, F_{prec} the rate of carbonate precipitation, γ the fraction of dead biomass transferred to the kerogen, τ_{bio} the residence time of carbon in the biosphere, Π_{bio} the productivity of the continental biosphere, and τ_{ker} the residence time of carbon in the kerogen. The accretion ratio, A, is defined as the fraction of seafloor carbonates accreted to the continents to the total seafloor carbonates. The regassing ratio, R, is defined as the fraction of seafloor carbonates regassed into the mantle to the total subducting carbonates. The values of the constants are summarised in Table 1.

Table 1. *Constants used in the carbon cycle model*

Constant	Value	Remarks
A	0.7	Accretion ratio
A_e	5.1×10^{14} m^2	Surface area of the Earth
A_o^*	3.63×10^{14} m^2	Present area of ocean basins
C_{tot}	7.4×10^{20} kg	Total mass of carbon in the system
f_c	0.194	Degassing fraction of carbon
g	9.81 m s^{-2}	Acceleration of gravity
$p_{1/2}$	210.8 ppm	Michaelis–Menten parameter
pH*	8.2	Present day ocean pH
p_{min}	10 ppm	Minimum CO_2 partial pressure allowing photosynthesis
R	0.7	Regassing ration
S_A^*	2.7 km^2 a^{-1}	Present day areal spreading rate
V_m	8.6×10^{20} m^3	Mantle volume
V_o	1.1687×10^{18} m^3	Volume of the ocean
λ	0.34 Ga^{-1}	Decay constant
μ_C	1.2×10^{-2} kg mol^{-1}	Transfer factor from mol to kg for carbon
μ_{CO_2}	4.4×10^{-2} kg mol^{-1}	Transfer factor from mol to kg for CO_2
Π_{max}	180×10^{12} kg a^{-1}	Maximum biosphere productivity
τ_f^*	77 Ma	Present day seafloor residence time
τ_{bio}	12.5 a	Residence time of carbon in the biosphere
τ_{ker}	1.58 Ga	Residence time of carbon in the kerogen

τ_f is the residence time of carbon in the seafloor and is parameterised with the help of the heat production rate, Q, according to Tajika and Matsui (1990):

$$\tau_f(t) = \frac{Q^*}{Q(t)} \sqrt{\frac{A_o}{A_o^*}} \cdot \tau_f^* = e^{\lambda(t-4.6\ \text{Ga})} \sqrt{\frac{A_o}{A_o^*}} \cdot \tau_f^*, \tag{7}$$

where Q^* is the present heat production rate of the mantle, A_o^* the present day area of the ocean basins,

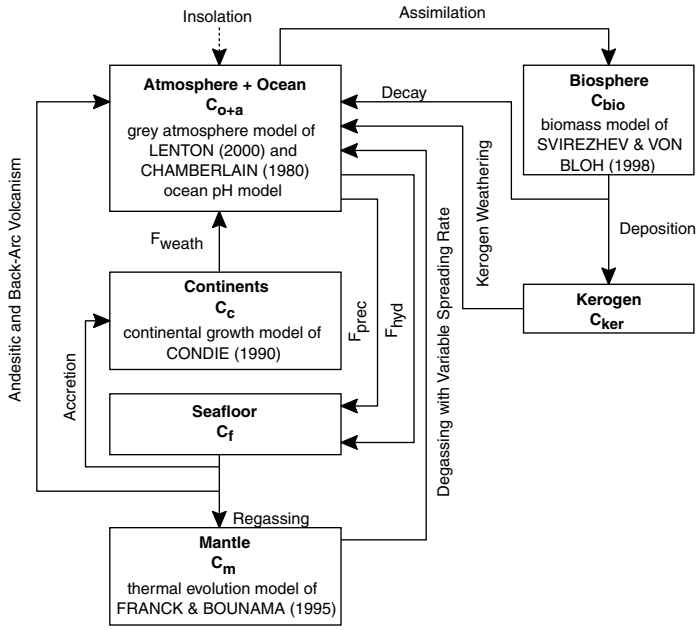

Fig. 1. Diagram illustrating the basic mechanisms and interactions of the global carbon cycle. The fluxes from and to the different pools are indicated by arrows.

τ_f^* the present seafloor residence time (Sprague and Pollack, 1980), and λ the decay constant (Table 1).

The total amount of carbon in the system, $C_{\rm tot}$, is conserved, i.e.

$$\frac{dC_m}{dt} + \frac{dC_{o+a}}{dt} + \frac{dC_c}{dt} + \frac{dC_f}{dt} + \frac{dC_{\rm bio}}{dt} + \frac{dC_{\rm ker}}{dt} = 0. \quad (8)$$

Therefore it is possible to reduce the set of equations for the global carbon cycle from six to five independent equations. The box model including the pertinent fluxes is sketchted in Fig. 1.

2.1. Thermal evolution model

To determine the thermal history and future of the Earth a parameterised model of whole mantle convection including the water exchange between mantle and surface reservoirs (Franck and Bounama, 1995; Franck, 1998) is applied. According to Allègre (1997) two-layer convection has operated for most of the Earth's history, but whole-mantle convection started less than 1 Ga ago. The assumption of whole-mantle convection is a first sufficient approximation with respect to our Earth system modelling.

Assuming conservation of energy we can write the following equation for the average mantle temperature, T_m:

$$\frac{4}{3}\pi\rho c\left(R_m^3 - R_c^3\right)\frac{dT_m}{dt} = -4\pi R_m^2 q_m + \frac{4}{3}\pi Q(t)\left(R_m^3 - R_c^3\right), \quad (9)$$

where ρ is the density, c is the specific heat at constant pressure, q_m is the heat flow from the mantle, Q is the energy production rate by decay of radiogenic heat sources in the mantle, and R_m and R_c are the outer and inner radii of the mantle, respectively.

The mantle heat flow is parameterised in terms of the Rayleigh number, Ra:

$$q_m = \frac{k(T_m - T_s)}{(R_m - R_c)}\left(\frac{Ra}{Ra_{\rm crit}}\right)^{\beta}, \quad (10)$$

with

$$Ra = \frac{g\alpha(T_m - T_s)(R_m - R_c)^3}{\kappa\nu}, \quad (11)$$

where k is the thermal conductivity, $Ra_{\rm crit}$ is the critical value of Ra for the onset of convection, β is an empirical constant, g is the acceleration of gravity, α is

the coefficient of thermal expansion, κ is the thermal diffusivity, and ν is the water-dependent kinematic viscosity. This viscosity can be calculated with the help of a water fugacity dependent mantle creep rate. For details of this parameterisation see Franck and Bounama (1995).

The evolution of the mass of mantle water, M_{mw}, is given as

$$\frac{\mathrm{d}M_{\mathrm{mw}}}{\mathrm{d}t} = f_{\mathrm{bas}}\rho_{\mathrm{bas}}d_{\mathrm{bas}}R_{\mathrm{H_2O}}(T_m)S_A - \frac{M_{\mathrm{mw}}}{V_m}d_m f_w S_A, \tag{12}$$

where f_{bas} is the water content in, ρ_{bas} is the average density of, and d_{bas} is the thickness of the basalt layer (ocean crust), $R_{\mathrm{H_2O}}$ is the regassing ratio of water, V_m is the volume of the mantle, and f_w is the outgassing fraction of water. The mass of water in the Earth system, M_{tot}, is constant over time, and therefore the mass of water in the surface reservoir can also be determined from the above equation. This value can be expressed as volume of the ocean. Estimations of the mantle water abundance range from 1.6 to 20 modern ocean masses, where one ocean mass is 1.404×10^{21} kg (Ringwood, 1975; Wänke et al., 1984; Liu, 1988; Ahrens, 1989; Jambon and Zimmermann, 1990; Smyth, 1994). Following McGovern and Schubert (1989) we assume 4 ocean masses of water in the entire system (of which one mass initially forms the surface reservoir). The areal spreading rate is a function of the average mantle temperature, the surface temperature, T_s, the mantle heat flow, and the continental growth model over the time-dependent area of ocean basins (Turcotte and Schubert, 1982):

$$S_A = \frac{q_m^2 \pi \kappa A_o(t)}{4k^2(T_m - T_s)^2}. \tag{13}$$

The area of ocean basins is parameterised with the help of the continental growth model of Condie (1990) and shown in Fig. 7b. This model is based on geochemical and geological data from the best studied region, North America and Europe. However, there is an ongoing discussion about continental growth scenarios stimulated by the recent discovery of evidence for some continental crust and a hydrosphere at 4.4 Ga from U–Pb dating of zircons with quartz inclusions (Wilde et al., 2001). The ideas that crustal volume has increased through time in spite of continental material being eroded and subducted back to the mantle, that the crustal growth rate was faster in the Archaean than today, and that crust formation ages tend to cluster around a small number of orogenic periods, have probably obtained the status of near-consensus (Albarède, 1998).

The variation of the regassing ratio with time is given as a function of average mantle temperature:

$$R_{\mathrm{H_2O}}(t) = m_{R_{\mathrm{H_2O}}}[T_m(0) - T_m(t)] + R_{\mathrm{H_2O}}(0), \tag{14}$$

where the factor $m_{R_{\mathrm{H_2O}}}$ is adjusted to get the correct present amount of surface water (one ocean mass) and $R_{\mathrm{H_2O}}(0)$ is fixed at 0.001, i.e. its value is very low at the beginning of the Earth's evolution because of the enhanced loss of water resulting from back-arc volcanism at higher temperatures.

For every time step we can determine the areal spreading rate, the melt generation depth, and the volume of the ocean with the help of the thermal evolution model. The thermal evolution is coupled to the carbon cycle via the surface temperature, which is only a tiny effect during most of Earth's history and future. The parameters used in the thermal evolution model are summarised in Table 2.

Table 2. *Constants used in the thermal evolution model*

Constant	Value	Remarks
d_{bas}	5×10^3 m	Average thickness of the basalt layer
f_{bas}	0.03	Mass fraction of water in the basalt layer
f_w	0.194	Degassing fraction of water
g	9.8 m s^2	Acceleration owing to gravity
k	4.2 J s^{-1} m^{-1} K^{-1}	Thermal conductivity
$M_{\mathrm{mv}}(0)$	4.212×10^{21} kg	Initial mass of mantle volatiles
Ra_{crit}	1100	Critical value of Ra for the onset of convection
R_c	3471×10^3 m	Inner radius of the mantle
R_m	6271×10^3 m	Outer radius of the mantle
$T_m(0)$	3000 K	Initial mantel temperature
α	3×10^{-5} K^{-1}	Coefficient of thermal expansion
β	0.3	Empirically determined dimensionless constant
κ	10^{-6} m^2 s^{-1}	Thermal diffusivity
ρ_{bas}	2950 kg m^{-3}	Density of the basalt
ρc	4.2×10^6 J m^{-3} K^{-1}	Density and specific heat

2.2. Atmospheric CO_2 partial pressure

The efficiency of weathering processes and the biosphere productivity strongly depend on the partial pressure of atmospheric CO_2, p_{CO_2}. Therefore, for each time step we calculate the equilibrium values of the mass of carbon in the ocean, C_o, and the atmosphere, C_a, to satisfy the condition $C_o + C_a = C_{o+a}$. This procedure requires the knowledge of the density profile of carbon dioxide above the surface. In the present version of the model we assume that the density of carbon dioxide in the atmosphere is constant versus elevation. In such a case the distribution of carbon can be calculated from the condition of equal partial pressures of CO_2 at the interface between atmosphere and ocean. The total mass of carbon in the ocean and in the atmosphere is

$$C_{o+a} = B p_{CO_2}, \tag{15}$$

where

$$B = \underbrace{\alpha_{H_2O} K_0 V_o(t) \left(\frac{1}{\gamma_{H_2CO_3}} + \frac{K_1}{a_{H^+} \gamma_{HCO_3^-}} + \frac{K_1 K_2}{a_{H^+}^2 \gamma_{CO_3^{2-}}} \right) \mu_C}_{C_o / p_{CO_2}} + \underbrace{\frac{A_e \mu_C}{g \mu_{CO_2}}}_{C_a / p_{CO_2}}. \tag{16}$$

K_0, K_1, and K_2 are equilibrium constants, and α_{H_2O}, $\gamma_{H_2CO_3}$, $\gamma_{HCO_3^-}$, and $\gamma_{CO_3^{2-}}$ activity coefficients (Table 3). A_e is the surface area of the Earth, g the acceleration of gravity, and $V_o(t) = [M_{tot} - M_{mw}(t)]/\rho_{H_2O}$ the volume of the ocean water, where ρ_{H_2O} is density of water (1000 kg m^{-3}). μ_C and μ_{CO_2} are molar masses (Table 3). The activity, a_{H^+}, of hydrogen ions is directly related to the pH of ocean water ($a_{H^+} = 10^{-pH}$) and is discussed in Section 2.5. The chemical parameters are taken from Tajika and Matsui (1990). Eqs. (15) and (16) allow us to calculate the partial pressure of atmospheric CO_2 from the value of C_{o+a}.

Table 3. *Constants in the weathering functions, equilibrium constants, and activity coefficients*

k_w^{cc}	175×10^{-5} Ma^{-1}	α_{H_2O}	0.967
k_w^{mc}	142×10^{-5} Ma^{-1}	$\gamma_{H_2CO_3}$	1.130
k_w^{cs}	28×10^{17} mol Ma^{-1}	$\gamma_{HCO_3^-}$	0.550
k_w^{ms}	31×10^{17} mol Ma^{-1}	$\gamma_{CO_3^{2-}}$	0.021
K_0	3.48×10^{-2} bar^{-1}	$\gamma_{Ca^{2+}}$	0.203
K_1	4.45×10^{-7} mol l^{-1}	$\gamma_{Mg^{2+}}$	0.260
K_2	4.69×10^{-11} mol l^{-1}		
k_{sp}^{cc}	3.60×10^{-9} mol^2 l^{-2}		
k_{sp}^{mc}	1.00×10^{-5} mol^2 l^{-2}		

2.3. Surface temperature

In order to calculate the surface temperature, T_s, we need a climate model which links the temperature to the given partial pressure of atmospheric CO_2 and the solar constant, S. Here we apply the grey atmosphere model of Lenton (2000) (see also Chamberlain, 1980). The temperature is determined using the energy balance between the incoming and outgoing radiation:

$$\sigma T_s^4 = \frac{(1-a)S}{4} \left(1 + \frac{3}{4}\tau \right), \tag{17}$$

where σ is the Stefan–Boltzmann constant (5.67×10^{-8} W m^{-2} K^{-4}), a is the average planetary albedo, and τ is the vertical opacity of the greenhouse atmosphere. The opacities of the two greenhouse gases, CO_2 and H_2O, are assumed to be independent from each other:

$$\tau = \tau \left(p_{CO_2} \right) + \tau \left(p_{H_2O} \right). \tag{18}$$

The opacity of CO_2 is assumed to be a function of its mixing ratio. It is derived from the results of varying CO_2 in a radiative–convective climate model (Kasting et al., 1993). The partial pressure of H_2O, p_{H_2O}, can be expressed as a function of temperature and relative humidity, H, using the Clausius–Clapeyron equation. Here we use a wet greenhouse model with $H = 1$ (full saturation). The albedo, a, is a function of the surface temperature (Caldeira and Kasting, 1992) derived from least-square fits to the results of a radiative–convective climate model with $0 \leq T_s\ ^\circ\text{C} \leq 100$:

$$a = 1.453\,614 - 0.006\,597\,9 T_s + 8.567 \times 10^{-6} T_s^2. \tag{19}$$

The opacities $\tau(p_{CO_2})$ and $\tau(p_{H_2O})$ are calculated in the following way:

$$\tau\left(p_{CO_2}\right) = 1.73\left(p_{CO_2}\right)^{0.263},$$
$$\tau\left(p_{H_2O}\right) = 0.0126\left(p_{H_2O}\right)^{0.503}. \quad (20)$$

The solar constant evolves according to Caldeira and Kasting (1992):

$$S(t) = S^*(1 - 0.38(t - 4.6\ \text{Ga})/4.55\ \text{Ga})^{-1}, \quad (21)$$

where S^* denotes the present-day value of the solar constant (1368 W m^{-2}).

Our climate model depends only on the brightening Sun and the CO_2/H_2O greenhouse effect. Therefore, we neglect so-called anti-greenhouse effects that potentially cool the planet: sulfuric acid aerosols (see, e.g., Peixoto and Oort, 1992), hydrocarbon stratospheric hazes (see e.g., Sagan and Chyba, 1997), ice–albedo feedbacks (see e.g., Kump et al. 1999), and clouds (see e.g., Kump et al., 1999).

2.4. Weathering

There are two main types of weathering processes: silicate weathering and carbonate weathering. First we describe the carbonate weathering, because it is the main process accounting for the flux of carbon from the continents to the ocean as described in eqs. (2) and (3). Silicate weathering is only important for the flux of CO_2 out of the combined "ocean + atmosphere" pool and does not influence the continental carbon reservoir. Therefore, it will be considered in the next section (precipitation). Our description of the weathering process is simplified in the sense of a minimal model. Detailed models of weathering reactions can be found in Berner et al. (1983), Berner (1994), and Berner and Kothavala (2001).

The rate of carbon transport from continents to the ocean driven by carbonate weathering is

$$F_{\text{weath}} = F^{\text{cc}}_{\text{weath}} + F^{\text{mc}}_{\text{weath}}, \quad (22)$$

where $F^{\text{cc}}_{\text{weath}}$ and $F^{\text{mc}}_{\text{weath}}$ are the weathering rates of $CaCO_3$ and $MgCO_3$, respectively. The weathering of calcium and magnesium carbonates is determined using the formulae given by Walker et al. (1981) and Caldeira and Kasting (1992):

$$F^{\text{cc}}_{\text{weath}} = k^{\text{cc}}_w \left(\frac{a_{H^+s}}{a^*_{H^+s}}\right)^{0.5} \exp\left(\frac{T_s - 288\ \text{K}}{13.7\ \text{K}}\right) C_c, \quad (23)$$

$$F^{\text{mc}}_{\text{weath}} = k^{\text{mc}}_w \left(\frac{a_{H^+s}}{a^*_{H^+s}}\right)^{0.5} \exp\left(\frac{T_s - 288\ \text{K}}{13.7\ \text{K}}\right) C_c. \quad (24)$$

The pre-factor outlines the role of CO_2 partial pressure in the soil, p_{soil}, a_{H^+s} is the activity of H^+ in fresh soil-water. The quantity $a^*_{H^+s}$ is the present value for the H^+ activity in the soil. The activity a_{H^+s} itself is a function of the surface temperature and the CO_2 partial pressure in the soil, where the equilibrium constants for the chemical activities of the carbon and sulfur systems have been taken from Stumm and Morgan (1981). p_{soil} depends on the terrestrial biological productivity per area, Π_A, the atmospheric CO_2 partial pressure, p_{CO_2}, and their corresponding (long-term mean pre-industrial) present values (p^*_{soil}, Π^*_A, $p^*_{CO_2}$):

$$\frac{p_{\text{soil}}}{p^*_{\text{soil}}} = \frac{\Pi_A}{\Pi^*_A}\left(1 - \frac{p^*_{CO_2}}{p^*_{\text{soil}}}\right) + \frac{p_{CO_2}}{p^*_{\text{soil}}}. \quad (25)$$

It is assumed that $p^*_{\text{soil}} = 10 p^*_{CO_2}$. The constants in the weathering functions, k^{cc}_w and k^{mc}_w, are shown in Table 3.

Our parameterisation of weathering that considers only the variation of soil carbon dioxide levels gives a biotic amplification of weathering of 1.56 for the present state (Lenton and von Bloh, 2001) which is a significant underestimate. Following Schwartzman (1999) the total weathering amplification due to land life is at least a factor of 10. This indicates that much of the observed biotic amplification of weathering is due to processes other than increased soil p_{CO_2}.

2.5. Precipitation

Weathering products are transported to the ocean and, depending on the solubility product, precipitated to the ocean floor. The rate of precipitation is

$$F_{\text{prec}} = \left(F^{\text{cc}}_{\text{weath}} + F^{\text{mc}}_{\text{weath}}\right) + \left(F^{\text{sc}}_{\text{weath}} + F^{\text{sm}}_{\text{weath}}\right)\mu_C - \left(\frac{\text{d}m^{\text{ca}}_{\text{eq}}}{\text{d}t} + \frac{\text{d}m^{\text{mg}}_{\text{eq}}}{\text{d}t}\right) V_{\text{shallow}}\mu_C. \quad (26)$$

V_{shallow} is the volume of shallow water in which precipitation to the seafloor can take place. According to Stacy (1992) 8% of the Earth's area is covered with ocean less shallow than 10^3 m, i.e. $V_{\text{shallow}} = 0.08 A_e 10^3$ m. This value is a first approximation, because the shallow ocean area might have changed during Earth's history. $F^{\text{sc}}_{\text{weath}}$ and $F^{\text{sm}}_{\text{weath}}$ are the weathering rates of $CaSiO_3$ and $MgSiO_3$. The biotic enhanced silicate weathering

rate is defined similar to the carbonate weathering [see eq. (24)]:

$$F^{\mathrm{sc}}_{\mathrm{weath}} = k^{\mathrm{cs}}_{w}\left(\frac{a_{\mathrm{H}^+ s}}{a^*_{\mathrm{H}^+ s}}\right)^{0.5} \exp\left(\frac{T_s - 288\ \mathrm{K}}{13.7\ \mathrm{K}}\right)\left(\frac{A_e - A_o}{A_e - A^*_o}\right), \tag{27}$$

$$F^{\mathrm{sm}}_{\mathrm{weath}} = k^{\mathrm{ms}}_{w}\left(\frac{a_{\mathrm{H}^+ s}}{a^*_{\mathrm{H}^+ s}}\right)^{0.5} \exp\left(\frac{T_s - 288\ \mathrm{K}}{13.7\ \mathrm{K}}\right)\left(\frac{A_e - A_o}{A_e - A^*_o}\right), \tag{28}$$

where k^{cs}_w and k^{ms}_w are given in Table 3.

$m^{\mathrm{ca}}_{\mathrm{eq}}$ and $m^{\mathrm{mg}}_{\mathrm{eq}}$ are the equilibrium concentrations of Ca and Mg cations in ocean water, which are always in a saturated state. The change of equilibrium concentrations results in a change of solubility of carbonates in ocean water and therefore influences the precipitation flux. The equilibrium concentrations of Ca and Mg cations are given by

$$m^{\mathrm{ca}}_{\mathrm{eq}} = \frac{k^{\mathrm{cc}}_{\mathrm{sp}}}{\gamma_{\mathrm{Ca}^{2+}} K_0 K_1 K_2 \alpha_{\mathrm{H_2O}}} \times \frac{a^2_{\mathrm{H}^+}}{p_{\mathrm{CO_2}}} = c_1 \times \frac{a^2_{\mathrm{H}^+}}{p_{\mathrm{CO_2}}}, \tag{29}$$

$$m^{\mathrm{mg}}_{\mathrm{eq}} = \frac{k^{\mathrm{mc}}_{\mathrm{sp}}}{\gamma_{\mathrm{Mg}^{2+}} K_0 K_1 K_2 \alpha_{\mathrm{H_2O}}} \times \frac{a^2_{\mathrm{H}^+}}{p_{\mathrm{CO_2}}} = c_2 \times \frac{a^2_{\mathrm{H}^+}}{p_{\mathrm{CO_2}}}, \tag{30}$$

where $k^{\mathrm{cc}}_{\mathrm{sp}}$ and $k^{\mathrm{mc}}_{\mathrm{sp}}$ are equilibrium constants and $\gamma_{\mathrm{Ca}^{2+}}$ and $\gamma_{\mathrm{Mg}^{2+}}$ are activity coefficients (Table 3).

Constant pH. According to Grotzinger and Kasting (1993) geological data do not confirm strong changes of pH. In our model we follow Caldeira and Berner (1999) and assume pH 8.2. The assumption of constant pH leads to the function

$$\frac{\mathrm{d}m^{\mathrm{ca}}_{\mathrm{eq}}}{\mathrm{d}t} + \frac{\mathrm{d}m^{\mathrm{mg}}_{\mathrm{eq}}}{\mathrm{d}t} = -\frac{B a^2_{\mathrm{H}+}(c_1 + c_2)}{C^2_{o+a}} \frac{\mathrm{d}C_{o+a}}{\mathrm{d}t}. \tag{31}$$

Time dependent pH. In this case we assume a simple quasi-stationary time dependence of the pH of the ocean in the following way:

$$\mathrm{pH(t)} = \begin{cases} t[\mathrm{pH}^* - \mathrm{pH}(t=0)]/4.6\ \mathrm{G}a + \mathrm{pH}(t=0) \\ \qquad\qquad\qquad \text{when} \quad t \le 4.6\ \mathrm{Ga} \\ \mathrm{pH}^* \qquad\qquad \text{when} \quad t > 4.6\ \mathrm{Ga} \end{cases}. \tag{32}$$

2.6. Hydrothermal reactions

Due to hydrothermal reactions CO_2 dissolved in the oceans reacts with fresh mid-ocean basalts and precipitates in the form of carbonates to the ocean floor. For the parameterisation of the hydrothermal flux, F_{hyd}, we use the following approximations:

Constant F_{hyd}. As a first approximation the hydrothermal flux is fixed to the present day value, F^*_{hyd}.

Spreading dependent F_{hyd}. As a second approximation it is assumed that the hydrothermal flux is proportional to the production of fresh basalt at mid ocean ridges, which in turn is proportional to the areal spreading rate:

$$F_{\mathrm{hyd}} = \left(S_A \,/\, S^*_A\right) F^*_{\mathrm{hyd}}, \tag{33}$$

where S^*_A is the present day areal spreading rate. In this case reaction kinetics is slow and limited by the abundance of cations.

Spreading and reservoir dependent F_{hyd}. Finally we follow Sleep and Zahnle (2001) and use the following formulation:

$$F_{\mathrm{hyd}} = \frac{S_A C_o}{A_{\mathrm{hydro}}}, \tag{34}$$

where A_{hydro} is 6×10^6 km^2. From the point of view of reaction kinetics this corresponds to fast reactions with a superabundance of cations.

2.7. Parameterisation of the biological productivity

The biological productivity per area, Π_A, is a function of surface temperature and CO_2 partial pressure of the atmosphere:

$$\Pi_A = \frac{\Pi_{\max}\Pi\left(T_s, p_{\mathrm{CO_2}}\right)}{A_e - A^*_o}, \tag{35}$$

where $\Pi(T_s, p_{\mathrm{CO_2}})$ is given by

$$\Pi(T_s, p_{\mathrm{CO_2}}) = \frac{p_{\mathrm{CO_2}} - p_{\min}}{p_{1/2} + p_{\mathrm{CO_2}} - p_{\min}} \times \left[1 - \left(\frac{T_s - 323\ \mathrm{K}}{50\ \mathrm{K}}\right)^2\right], \tag{36}$$

and $\Pi_{\max}$ is the maximum biological productivity of the present continental area. It is assumed to be twice the present day productivity. Outside the temperature tolerance window between 273 K and 373 K Π is set

to zero. For the dependence on the partial pressure of atmosphere CO_2 we have a Michaelis–Menten hyperbola with saturation, while for the dependence on temperature a parabolic form is assumed. The parameter $p_{\min}$ is the minimum CO_2 partial pressure allowing photosynthesis and $p_{1/2} + p_{\min}$ is the pressure corresponding to the productivity of the biosphere two times smaller than its maximum value. The values are given in Table 1.

The biological productivity is then calculated as

$$\Pi_{\text{bio}} = \Pi_A(A_e - A_o). \tag{37}$$

2.8. Kerogen cycle

Kerogen is probably the least important reservoir from the point of view of carbon cycling because it is relatively inert. However, there are processes of kerogen weathering and kerogen formation. The present size of the kerogen reservoir of 10–20% of the surface reservoirs is obviously the net result of these processes. The main constraint for the reservoir size results from isotopic geochemistry. Since kerogen is isotopically light due to its biological origin it preferentially sequestors ^{12}C, while the continental carbon reservoir must get enriched in the heavier isotope ^{13}C. The isotopic composition of the two carbon reservoirs kerogen and continental crust might have been constant over the last 3.5 Ga (Junge et al., 1975; Schidlowski, 1988). The ratio of kerogen carbon to continental carbon would also have been constant at a value of 1:4, taking into account the isotopic signature of the mantle carbon. Based on this, we can determine the up-to-now unknown parameters of the fraction of dead biomass transfer, γ, and the residence time of carbon in the kerogen, τ_{ker}. The condition that $\gamma < 1$ sets a lower limit of τ_{ker}. The values for γ and τ_{ker} are chosen in such a way that C_c/C_{ker} remains roughly constant at the above given value.

In summary, the final minimal model consists of six dynamical equations for the global carbon cycle [eqs. (1)–(6)], one equation for the thermal evolution of the Earth [eq. (9)], and one equation for the water degassing evolution [eq. (12)]. All equations are coupled through nonlinear feedback mechanisms and have to be solved simultaneously. Due to very different time scales of the incorporated processes a stiff equation solver for ordinary differential equations is used to run the model from 4.6 Ga ago up to 2 Ga into Earth's future.

3. Results and discussion

As already mentioned in the model description, our model contains the cycling of the two main volatiles in the Earth system: water and carbon dioxide. While the mantle water content has the main influence on the mantle rheology and on the volatile exchange between mantle and surface reservoirs, the atmospheric carbon dioxide content is the main factor determining the climate. The total amount of both volatiles is a topic of ongoing controversial discussion. There are certain estimates of the total amount of water in the Earth system based on geochemical investigations and/or accretion models (see Franck and Bounama, 2001). In the present paper, the thermal evolution model is based on a total amount of four ocean masses of water in the Earth system, i.e. at present there are three ocean masses of water in the mantle and one at the surface. The total amount of carbon at the Earth's surface has been estimated by various geochemical studies. The "classical" value of 1.2×10^{20} kg(C) is given by Ronov and Yaroshevsky (1976). The mantle carbon content was calculated by Tajika and Matsui (1992) from recent estimates of CO_2 degassing at mid-ocean ridges to be more than five times the present amount of surface carbon. Following this, we use 7.4×10^{20} kg(C) as the reference value for the total carbon content.

3.1. Variation of initial conditions

For the thermal evolution model we assume an average mantle temperature of $T_m(0) = 3000$ K as initial condition. The initial amount of mantle water is set to $M_{\text{mw}}(0) = 3$ ocean masses. Both initial values are not varied. An analysis of a variation of $T_m(0)$ can be found in Franck and Bounama (1995, 1997) and Franck (1998). Different initial distributions of water as the main volatile between mantle and surface reservoirs in the Earth system have been studied in Franck and Bounama (2001). Following the standard case of Tajika and Matsui (1992) we begin with 80% of total carbon in the surface reservoirs:

$$C_m(0) = 0.2C_{\text{tot}},$$

$$C_{\text{o+a}}(0) = C_f(0) = 0.4C_{\text{tot}},$$

$$C_c(0) = C_{\text{bio}}(0) = C_{\text{ker}}(0) = 0,$$

where C_{tot} is the total amount of carbon in the system. The general knowledge about the initial distribution of

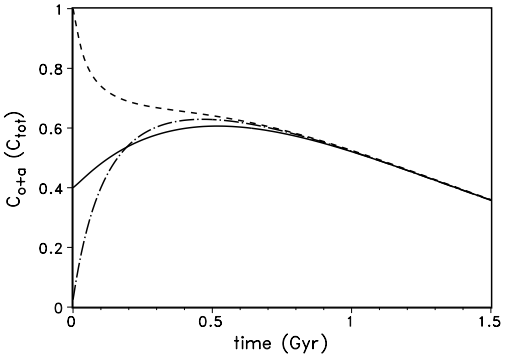

Fig. 2. Evolution of the combined ocean and atmosphere reservoir, $C_{\mathrm{o+a}}$, scaled to the total amount of carbon, C_{tot}, for various initial distributions of carbon between the pools. Note that after 1 Ga the system has "forgotten" the initial conditions.

carbon is rather poor. There are some hints from planetogonic scenarios that take into account the distribution coefficient of CO_2 between the early atmosphere and the magma ocean (Abe, 1988), but such estimations are far from being definitive. Therefore, we start our calculations with a comparison of the temporal variations of the combined ocean–atmosphere reservoir for three different starting conditions: $C_{\mathrm{o+a}} = 0.025C_{\mathrm{tot}}$ ($C_m = 0.95C_{\mathrm{tot}}$, $C_f = 0.025C_{\mathrm{tot}}$), $C_{\mathrm{o+a}} = 0.40C_{\mathrm{tot}}$ (see above), and $C_{\mathrm{o+a}} = 1.00C_{\mathrm{tot}}$. As shown in Fig. 2, all three curves converge after about 1 Ga, i.e. the Earth system has "forgotten" its initial conditions. No matter how carbon was distributed 4.6 Ga ago, the system would arrive at the same state today. This effect is called adjustment, and it has also been observed in various other reservoirs.

3.2. *Model results for the thermal and degassing evolution*

In Fig. 3 the evolution of the average mantle temperature, T_m, and of the surface water reservoir, M_{surf}, are shown. We find a secular mantle cooling of about 250 K in the last 3 Ga. This is in good agreement with melting experiments of komatiite liquids (Herzberg, 1995). The curve of M_{surf} shows an outgassing event at the beginning of planetary evolution followed by a subsiding process to end up in the recent situation of one ocean at the Earth's surface. Such an outgassing event in early Earth history is proved by geochemical data of noble gas depletion ratios (Staudacher and Allègre, 1982).

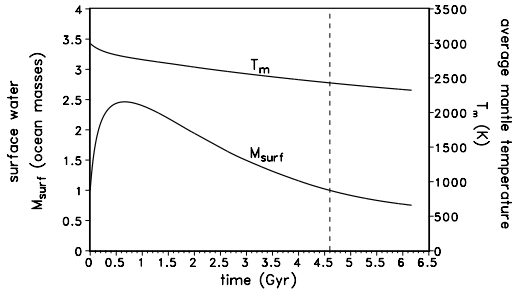

Fig. 3. Evolution of the average mantle temperature, T_m, and the surface water reservoir, M_{surf}, derived from the thermal evolution model.

3.3. *Model results for constant hydrothermal flux*

Here we restricted ourselves to the case in which hydrothermal carbonatisation (F_{hyd}) is always constant at the present value. The different results for the present reservoir sizes are given in Table 4. In this table the results of other authors are also displayed, and we find general agreement to a great extent. In Table 5 the present-day values of the mantle fluxes for carbon and water, the melting depth, the spreading rate, and the net fluxes of all carbon reservoirs are shown and compared to available data.

Evolution of reservoirs. A main outcome of our modelling is the evolution of the carbon content in the six reservoirs mantle, ocean + atmosphere, ocean floor, continents, biosphere, and kerogen (Fig. 4a). One can distinguish three different periods: from Earth's origin to the onset of continental growth at 1.5 Ga, from 1.5 Ga until the present, and from the present into the future. In the Hadean and early Archaean periods we have no noticeable continental area and therefore no continental biosphere and no kerogen. There is no weathering and most of the carbon is in the coupled ocean–atmosphere pool. With the beginning of continental growth at about 1.5 Ga we observe a strong decrease of the ocean and atmosphere pool and a strong increase of the ocean floor pool as a result of the onset of weathering. Later on the ocean floor pool decreases steadily. Only the mantle carbon pool increases monotonously. The increase in the continental pool reflects the episodes of strong continental growth. The kerogen pool is rather small, but increases up to about 16% of the present surface reservoirs. In the future this pool will decrease as a result of decreasing kerogen deposition.

Evolution of kerogen. The residence time of carbon in the kerogen pool was chosen (Table 1) to maintain

Table 4. *Present day ($t = 4.6$ Ga) values of reservoir sizes in fraction of the total amount of carbon in the system ($C_{tot} = 7.4 \times 10^{20}$ kg), atmospheric CO_2 partial pressure of the atmosphere, surface temperature, and lifespan of the biosphere for three parameterisations of the hydrothermal flux: (I) $F_{hyd}(t) = F^*_{hyd}$, (II) $F_{hyd}(t) \sim S_A$, (III) $F_{hyd}(t) \sim S_A C_o$, with three models for the ocean pH evolution: (a) $pH(t) + 8.2 + pH^*$, (b) initial "acid ocean" pH(0) = 6.5, and (c) initial "soda ocean" pH(0) = 10.5*

Model[a]	C_m	C_{o+a} (10^{-5})	C_c	C_f	C_{bio} (10^{-7})	p_{CO_2} (10^{-6} bar)	T_s (K)	Life-span (Ga)
(Ia) $\gamma = 0$ no biosphere $m_{R_{H_2O}} = 6.76 \times 10^{-4}$	0.87	4.1	0.10	0.027	–	339	288.6	–
(Ia) $\gamma = 0$ no kerogen $R_{H_2O} = 6.76 \times 10^{-4}$	0.87	3.1	0.10	0.028	7.8	260	286.8	5.82
(Ia) $\gamma = 1.95 \times 10^{-4}$ $m_{R_{H_2O}} = 6.76 \times 10^{-4}$	0.85	3.1	0.10	0.028	7.8	261	286.8	5.83
(IIa) $\gamma = 2.36 \times 10^{-4}$ $m_{R_{H_2O}} = 6.75 \times 10^{-4}$	0.83	3.1	0.11	0.030	7.7	257	286.7	5.85
(IIIa) $\gamma = 5.70 \times 10^{-3}$ $m_{R_{H_2O}} = 6.54 \times 10^{-4}$	0.63	1.0	0.28	0.032	2.2	84	280.6	5.89
(Ib) $\gamma = 1.87 \times 10^{-4}$ $m_{R_{H_2O}} = 6.79 \times 10^{-4}$	0.85	3.0	0.10	0.026	7.4	248	286.5	5.83
(IIb) $\gamma = 2.28 \times 10^{-4}$ $m_{R_{H_2O}} = 6.78 \times 10^{-4}$	0.84	2.9	0.11	0.028	7.3	242	286.3	5.85
(IIIb) $\gamma = 5.48 \times 10^{-4}$ $m_{R_{H_2O}} = 6.60 \times 10^{-4}$	0.75	3.3	0.17	0.043	8.1	273	287.1	5.88
(Ic) $\gamma = 2.16 \times 10^{-4}$ $m_{R_{H_2O}} = 6.52 \times 10^{-4}$	0.81	3.7	0.12	0.037	9.0	309	288.0	5.84
(IIc) $\gamma = 2.41 \times 10^{-4}$ $m_{R_{H_2O}} = 6.52 \times 10^{-4}$	0.80	3.6	0.13	0.037	8.8	299	287.8	5.85
(IIIc) $\gamma = 8.04 \times 10^{-2}$ $m_{R_{H_2O}} = 6.50 \times 10^{-4}$	0.59	3.5	0.32	0.020	3.3	29	276.6	5.74
Values given in other publications	0.83	5.4[b,c]	0.12[d]	0.030[d]	8.1[c]	220[e]–240[f]		

[a] γ is chosen to get $C^*_{ker}/C^*_c = 0.25$. $m_{R_{H_2O}}$ is adjusted to get one ocean mass of surface water.
[b] Holland (1978).
[c] Kasting and Walker (1992).
[d] Ronov and Yaroshevsky (1976).
[e] Falkowski et al. (2000).
[f] Pearson and Palmer (2000).

a roughly constant ratio C_{ker}/C_c. In all calculations γ [eq. (6)] has to be adjusted to give this recent ratio of 0.25. The evolution of the ratio C_{ker}/C_c is shown in Fig. 4b. One can distinguish three different regimes. With the beginning of continental growth (and the appearance of the terrestrial biosphere) the graph shows a pronounced spike caused by the different characteristic time scales of the dynamics of C_c and C_{ker}. After this the ratio remains roughly constant around the observed value of 0.25. Undulations are related to the episodes of rapid continental growth. After 5.5 Gyr the ratio increases rapidly connection with the breakdown of the carbon cycle.

Evolution of p_{CO_2}. Figure 4c shows the evolution of the atmospheric CO_2 content. As expected from the general effect of self-stabilisation in the Earth system under the influence of increasing insolation, we find monotonous decrease of p_{CO_2} over more than 6 Ga. The strong decrease after 1.5 Ga is related to the continental growth model of Condie (1990), with episodic growth and certain maxima of growth rates and the connected increase of weathering. Alternative models without episodic continental growth would generally

Table 5. *Present day model results for constant hydrothermal flux*

Model variable	Numerical value	Comparison
Subducting flux of H_2O, F_{reg}	1.21×10^{12} kg a^{-1}	$(0.9-1.9) \times 10^{12}$ kg a^{-1} (Bebout, 1996)
Recycling flux of H_2O, F_{cyc}	0.74×10^{12} kg a^{-1}	$(0.85-0.95) \times 10^{12}$ kg a^{-1} (Bebout, 1996)
Melting depth, d_m	56.5 km	56 km (Langmuir et al., 1992)
Spreading rate, S_A	2.73 km^2 a^{-1}	2.84 km^2 a^{-1} (Turcotte and Schubert, 1982)
Carbon flux into the mantle, F_{in}	5.6×10^{10} kg a^{-1}	$(6.1-27.9) \times 10^{10}$ kg a^{-1} (Bebout, 1996)
Carbon flux from the mantle, F_{out}	3.6×10^{10} kg a^{-1}	2.7×10^{10} kg a^{-1} (Bebout, 1996)
dC_m/dt	2.0×10^{10} kg a^{-1}	
dC_{o+a}/dt	-9.3×10^{7} kg a^{-1}	
dC_c/dt	2.9×10^{9} kg a^{-1}	
dC_f/dt	-1.8×10^{10} kg a^{-1}	
dC_{bio}/dt	-9.3×10^{5} kg a^{-1}	
dC_{ker}/dt	-5.5×10^{9} kg a^{-1}	

result in smooth surface temperature curves. The strong decrease after 1.5 Ga would vanish if there were a remarkable continental area on early Earth. An increase of continental area will principally result in a decrease of T_s. Similar investigations concerning the tectonic control of geochemical cycles have been performed by Godderis and Veizer (2000). They exclude also a so-called 'big bang' scenario for

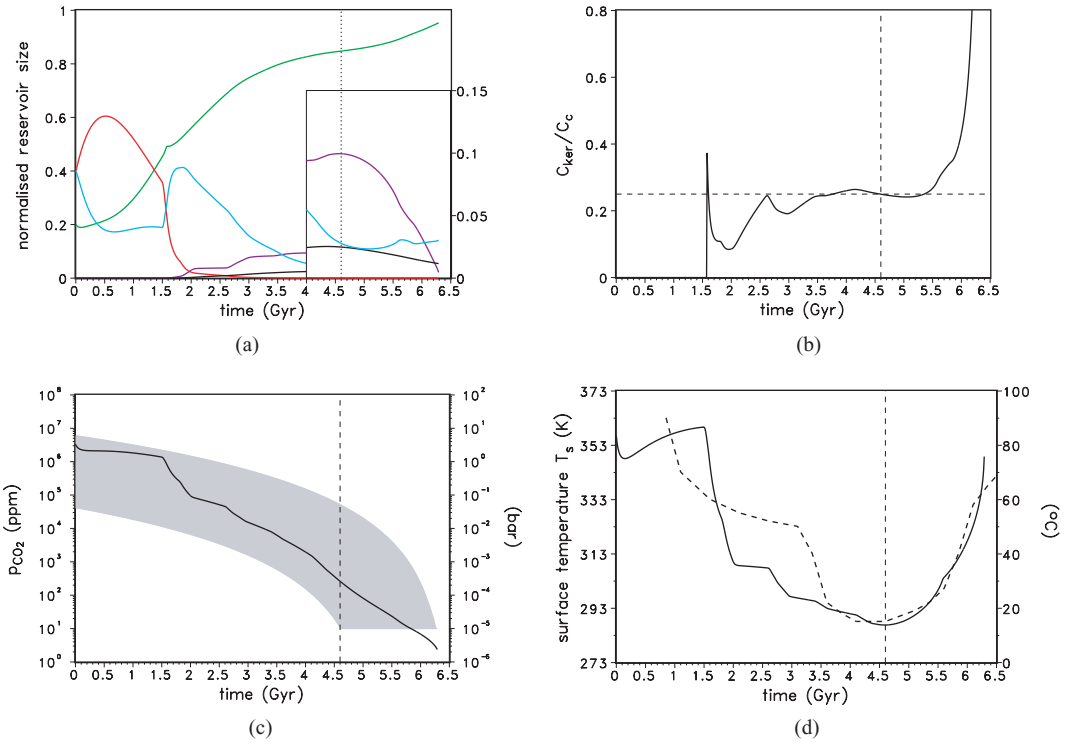

Fig. 4. Model results for constant hydrothermal flux: (a) evolution of the reservoirs mantle (green), atmosphere + ocean (red), ocean floor (blue), kerogen (black), and continents (magenta), (b) evolution of the ratio C_{ker}/C_c where the horizontal dashed line indicates the observed ratio of 0.25, (c) evolution of atmospheric partial pressure of carbon dioxide, p_{CO_2}, where the grey shaded area represents values for non-vanishing biological productivity, and (d) evolution of the surface temperature, T_s, where the dashed line indicates the result of Schwartzman (1999) (Fig. I–I, p. 2).

continental generation shortly after the accretion of Earth and found a strong influence of episodes with high continental growth rates on geochemical cycles. The atmospheric CO_2 content always stays in an interval maintaining the temperatures in the tolerance window [0 °C; 100 °C]. In the first 3.5 Ga of Earth's history p_{CO_2} is higher than about 10^4 ppm (10^{-2} bar), which is in contradiction to results from the investigation of paleosoils (Rye et al., 1995). A solution to this problem would be the introduction of a carbon cycle model with strongly enhanced hydrothermal reactions (Sleep and Zahnle, 2001). Nevertheless, this p_{CO_2} limit has been challenged (Schwartzman, 1999; Ohmoto et al., 2001). The atmospheric CO_2 content of the present model is about 261 ppm (2.61×10^{-4} bar). This is in agreement with the average atmospheric CO_2 concentration during the past 420 ka, which was only ≈220 ppm, and the pre-industrial level of 280 ppm (Falkowski et al., 2000). There are also other hints that the average carbon dioxide concentration was also in this range during the last 20 Ma (Pearson and Palmer, 2000). On longer time scales, however, the paleoatmospheric CO_2 levels indicate large fluctuations. According to Ekart et al. (1999) carbon dioxide levels increased through the Triassic period to approximately 3000 ppm, and dropped to less than 1000 ppm prior to the Cretaceous–Tertiary boundary, while relatively low levels persisted throughout the Cenozoic. Our model gives a maximum value of about 600 ppm in the Mesozoic. About 1.2 Ga in the future, the atmospheric CO_2 content becomes lower than 10 ppm (10^{-5} bar), and this state marks the end of the life-span of the biosphere.

Evolution of surface temperature. Our model results for the long-scale evolution of the mean global surface temperature are shown in Fig. 4d, in comparison with the results of Schwartzman (1999). The Hadean and early Archaean is characterised by rather high temperatures near to 353 K. The start of continental growth results in a strong temperature decrease caused by the "onset" and increase of weathering. We can even identify periods of strongly enhanced continental growth rates. It is very interesting that the present epoch seems to be the moment in Earth's history at which the global surface temperature is at a minimum value. In the long-term future the self-regulation process can not balance the increasing insolation and therefore temperature will become very high in less than 2 Ga. After 3.6 Ga in to the future there is a very good agreement of our model results with those of Schwartzman (1999). Before 3.6 Ga there is only a qualitative agreement, namely a cooling. This deviation results primarily from the underestimation of the amplification of weathering by biota. Following Lenton and von Bloh (2001) the weathering functions [eqs. (23), 24, (27), and (28)] can be altered to include a direct dependence of the weathering rate on productivity with an amplification factor α, which gives, e.g., the modified carbonate weathering rate, F'_{weath}:

$$F'_{\text{weath}} = \left[\left(1 - \frac{1}{\alpha}\right)\frac{\Pi_A}{\Pi_A^*} + \frac{1}{\alpha}\right]\left(F^{\text{cc}}_{\text{weath}} + F^{\text{mc}}_{\text{weath}}\right). \tag{38}$$

For $\alpha = 1$ eq. (38) is identical to eq. (22). The variation of α combined with different temperature tolerance windows for the biota [eq. (36)] gives a tool to describe the Archaean and Proterozoic biosphere in a more detailed way. Here we restrict ourselves to an aggregated biosphere model. Dividing the biosphere

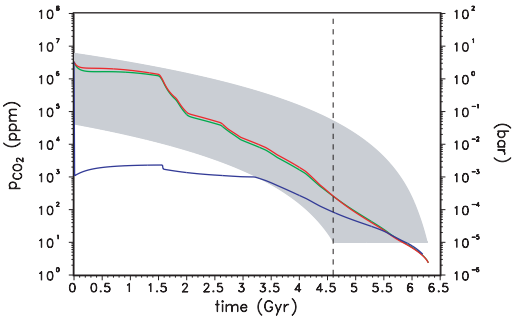

(a)

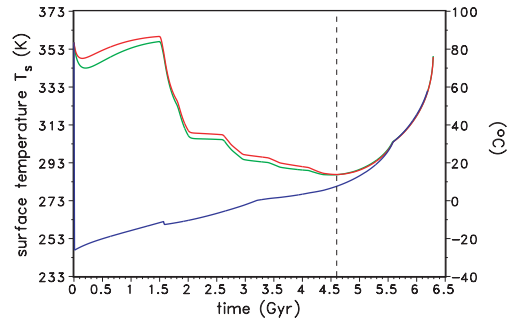

(b)

Fig. 5. Evolution of atmospheric CO_2 partial pressure, p_{CO_2}, where the grey shaded area represents values for non-vanishing biological productivity (a) and surface temperature, T_s, (b) for three different parameterisations of the hydrothermal flux: constant (red), slow hydrothermal reaction kinetics (green), fast hydrothermal reaction kinetics (blue).

pool into different types will be the topic of future investigations.

3.4. Parameterisation of the hydrothermal flux

In Fig. 5a we have plotted the evolution of atmospheric carbon dioxide concentration for the three different parameterisations of the hydrothermal flux described previously. It is obvious that the curves for the constant F_{hyd} and the spreading dependent F_{hyd} (slow hydrothermal reaction kinetics) do not differ significantly. Thus, the discussion given with Fig. 4c also refers to the model with spreading dependent F_{hyd}. On the other hand, the formulation of Sleep and Zahnle (2001), with fast reaction kinetics, gives qualitatively different results for the whole of Earth's history. In this case hydrothermal carbonatisation works so effectively in the past that the atmospheric carbon dioxide concentration is nearly constant over the last 4.6 Ga and the greenhouse effect of CO_2 can not balance the faint young Sun. This is also manifestedc in the evolution of the mean global surface temperature (Fig. 5b), which is outside the tolerance window in the first 3.3 Ga. The assumption of fast reaction kinetics for hydrothermal carbonatisation allows a freezing Hadean climate. To provide Archaean and Proterozoic long-term surface temperatures above the freezing point of water it is necessary to include other greenhouse gases in addition to water and carbon dioxide.

3.5. Different ocean pH evolution models

As first pointed out by Walker (1985), the pH of ocean water is the main factor in controlling the partition of CO_2 between the ocean and the atmosphere in the combined ocean + atmosphere reservoir. In Fig. 6a the evolution of the atmospheric carbon dioxide concentration is shown for three different pH scenarios

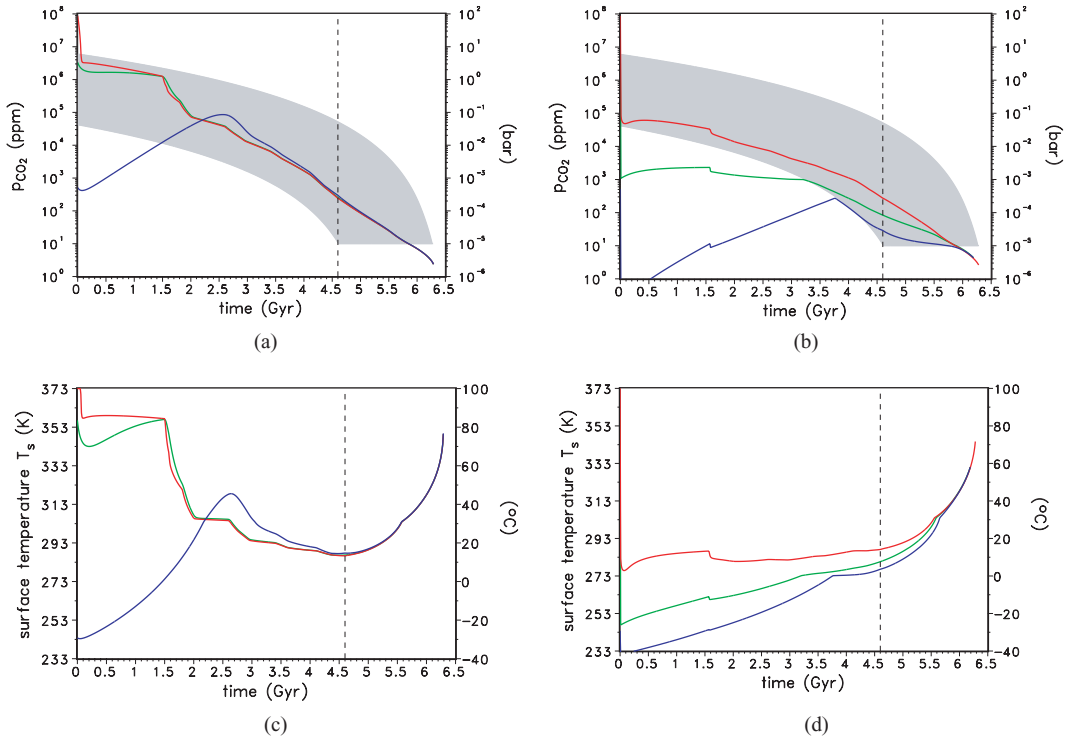

Fig. 6. Evolution of atmospheric CO_2 partial pressure, p_{CO_2}, where the grey shaded area represents values for non-vanishing biological productivity (a, b) and surface temperature, T_s, (c, d) under the condition of slow hydrothermal reaction kinetics (a, c) and fast hydrothermal reaction kinetics (b, d) for three different ocean pH models: acid ocean model (red), constant pH (green), and soda ocean model (blue).

with a spreading dependent hydrothermal flux (slow reaction kinetics): constant pH over Earth's history, i.e. $pH(t) = 8.2 = pH^*$, an acid ocean, i.e. $pH(0) = 6.5$, and a soda ocean in the past, i.e. $pH(0) = 10.5$. In the geological past the model results with constant pH and an initial acid ocean do not differ significantly. In the case of an initial soda ocean we find much lower values for p_{CO_2} in the past. Up to now there is no consensus about the oceanic pH in the past. It is well known that both alkaline and acid waters can be produced as a function of low-temperature reactions or high-temperature hydrothermal circulation, respectively (Sleep and Zahnle, 2001). Back to the Precambrian, geological arguments favour an almost constant oceanic pH (Grotzinger and Kasting, 1993). The oceanic pH of the Archaean and Paleoproterozoic need not have been significantly different from the modern value. Higher CO_2 partial pressures in the order of *1* bar require somewhat lower pH values down to around 6 (Grotzinger and Kasting, 1993). As we can see in Fig. 6c, the soda ocean scenario favoured by Kempe and Degens (1985) provides freezing Hadean and early Archaean surface temperatures unless there are other greenhouse gases acting in the atmosphere. The data for different pH scenarios and a hydrothermal flux with fast reaction kinetics (Sleep and Zahnle, 2001) shown in Fig. 6b give acceptable results only in the case of acid pH. The other two scenarios are connected with temperatures in the past that were too low. Figures 6c and 6d contain the resulting surface temperatures from the applied greenhouse model.

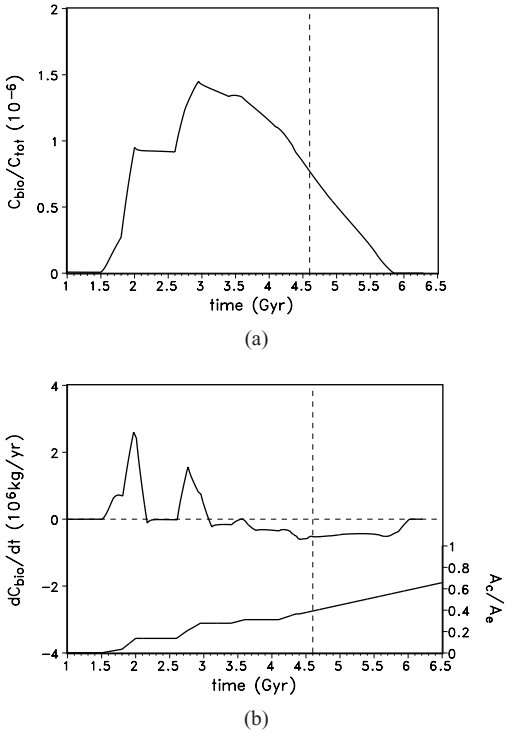

Fig. 7. Evolution of the biosphere pool, C_{bio}, (a) and its time derivative, dC_{bio}/dt, (b) for slow hydrothermal reaction kinetics to emphasise changes in the biosphere pool. In order to demonstrate the correlation between the continental growth rate and changes in the biosphere pool the Condie model (Condie, 1990) is displayed additionally in (b).

3.6. Influence of biosphere and kerogen

The question of how much biomass exists at different stages in the Earth's evolution is of great relevance for our modelling. Up to now it is difficult to obtain hard quantitative data on the biomass at any given time in Earth's history. There are divergent hypotheses (see, e.g., Glaessner and Foster, 1992) as to whether there was a significant increase in biomass since the early Precambrian period or not. Our model results sketched in Fig. 7a show a strong increase in continental biomass starting with the continental growth, and a maximum biomass in the Mesoproterozoic. Since this time there is an almost linear decrease up to the end of the biosphere's life span in about 1.2 Ga. At this point we should reflect on our formulae for the biological productivity [eqs. (35)–(37)]. Based on this, the terrestrial biomass is greater the higher the atmospheric carbon dioxide content, the closer the surface temperature to its optimum value of 50 °C, and the larger the continental area. Only with respect to these conditions can we understand the temporal behaviour of C_{bio}/C_{tot}. Our results seem to contradict the findings of Berner (1993) on the boost of terrestrial biomass given by the rise of higher plants in the Paleozoic. This might be solved by the introduction of different biosphere types into the model. In Fig. 7b the continental growth model and the time derivative of C_{bio} are plotted over time. There is an obvious correlation between episodes of enhanced continental growth and high positive values of dC_{bio}/dt. The peaks in the derivative dC_{bio}/dt are specifically for the Condie continental growth model and typically for orogenic periods of crust formation. The absolute minimum of this derivative can be found near to the present geological time.

The influence of the biosphere on the mean global surface temperature is shown in Fig. 8, where the

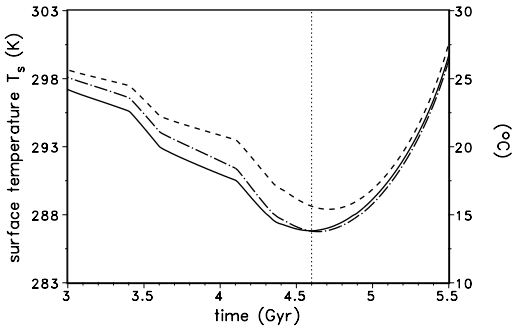

Fig. 8. Evolution of the global mean surface temperature, T_s, around present showing the cooling effect of the biosphere and the kerogen. The dashed line denotes the model results for constant hydrothermal flux without biosphere, the dashed–dotted one with biosphere but without kerogen, and the solid line the full model.

results for three different models are plotted: the full model (with biosphere and kerogen pool), a model with biosphere but without kerogen pool, and a model without biosphere (and therefore also without kerogen pool). The cooling of the biosphere (see, e.g., Lenton, 2001) is clearly shown: in the presence of a biosphere and kerogen pool the surface temperature is always lower than in the abiotic case. At present, the cooling is about 1.8 K. This is mainly caused by the biotic enhancement of weathering. The present geological epoch is characterised by the lowest global mean surface temperatures and a remarkable biosphere cooling. This is a further hint that the present state of the ecosphere is at the optimum in the sense that the present state is most favourable for the emergence of higher life forms, including intelligence (Schwartzman and Middendorf, 2000).

4. Conclusions

We have investigated the global carbon cycle coupled to the thermal and degassing evolution from the origin of the Earth up to 2 Ga into the future.

Studying different initial distributions of carbon between the reservoirs we find that for all scenarios the system forgets its initial conditions after about 1 Ga. This is an "adjustment" effect analogously found in mantle thermal evolution models (Schubert, 1979; Christensen, 1985). In most cases at present the surface temperature is at a minimum. The Earth system is at a point of evolution where the external forcing of increasing insolation takes over the main geodynamic influences, i.e. spreading, continental area, seafloor residence time of carbon, and melt generation depth. In the long-term future increasing insolation causes a breakdown of self-regulation, and the temperature rises above the upper boundary of the temperature tolerance window for vegetation. In our model, the life-span of the biosphere is determined by a lack of CO_2 1.2 Ga in the future. However, there could exist anti-greenhouse effects like aerosols, stratospheric hazes, and clouds that influence climate apart from the global carbon cycle, possibly extending the life-span. It is interesting that the present state of the Earth system is characterised not only by a minimum in surface temperature, but also by a minimum of the time derivative of the biosphere pool, i.e. the Earth system is just at the inflection point of the function $C_{\mathrm{bio}}(t)$ (Figs. 7a, and b).

The two scenarios with constant hydrothermal flux and slow reaction kinetics ($F_{\mathrm{hyd}} \sim S_A$) always give similar results, while the scenario with fast reaction kinetics ($F_{\mathrm{hyd}} \sim S_A C_o$) gives an icehouse up to the Archaean period. In the latter case temperatures are lower than in the others up to the present time, and all cases converge in the planetary future. Thus, again the present state of the Earth system seems to be special.

The investigations of different pH scenarios show the strong interplay between hydrothermal carbonatisation and ocean pH history: the scenario with fast reaction kinetics coupled to an acid ocean results in surface temperatures that are rather low but always above freezing for the whole of Earth's history and future.

Answering the question about the present state of the ecosphere we conclude: the 4.6-Ga-old Earth system today is operating in an optimum manner of self-regulation for higher life forms. On a planetary time-scale, however, the future regulation performance degradates up to a complete breakdown due to our maturing Sun.

5. Acknowledgements

This work was supported by the German Science Foundation (DFG, grant number IIC5-Fr910/9-4), the Federal Government and the Länder agreement (HSPN, grant number 24-04/235;2000), a project of scientific–technological cooperation with Poland (grant number POL-199-96), and the Polish State Committee for Scientific Research (KBN). We would like to thank the three reviewers for their constructive remarks.

REFERENCES

Abe, Y. 1988. Abundance of carbon in an impact-induced proto-atmosphere. *Proc. 21st ISAS Lunar Planet. Symp.* 238–244.

Ahrens, T. J. 1989. Water storage in the mantle. *Nature.* **342**, 122–123.

Albarède, F. 1998. The growth of continental crust. *Tectonophysics* 296,1–14.

Allègre, C. C. 1997. Limitation on the mass exchange between the upper and lower mantle: the evolving convection regime of the Earth. *Earth Planet. Sci. Lett.* **150**, 1–6.

Bebout, G. E. 1996. Volatile transfer and recycling at convergent margins: mass-balance and insights from high-P/T metamorphic rocks. *Geophys. Monogr.* **96**, 179–193.

Berner, R. A. 1993. Paleozoic atmospheric CO_2: importance of solar radiation and plant evolution. *Science* **261**, 68–70.

Berner, R. A. 1994. GEOCARB II: A revised model of atmospheric CO_2 over Phanerozoic time. *Am. J. Sci.* **294**, 56–91.

Berner, R. A. and Kothavala, Z. 2001. GEOCARB III: A revised model of atmospheric CO_2 over Phanerozoic time. *A. J. Sci.* **301**, 182–204.

Berner, R. A., Lasaga, A. C. and Garrels, R. M. 1983. The carbonate-silicate geochemical cycle and its effect on atmospheric carbon dioxide over the past 100 million years. *Am. J. Sci.* **283**, 641–683.

Bounama, C., Franck, S. and von Bloh, W. 2001. The fate of Earth's ocean. *Hydrol. Earth Syst. Sci.* **5**, 569–575.

Caldeira, K. and Kasting, J. F. 1992. The life span of the biosphere revisited. *Nature* **360**, 721–723.

Caldeira, K. and Berner, R. 1999. Seawater pH and atmospheric carbon dioxide. *Science* **286**, 2043a.

Chamberlain, J. W. 1980. Changes in the planetary heat balance with chemical changes in air. *Planet. Space Sci.* **28**, 1011–1018.

Christensen, U. R. 1985. Thermal evolution models for the Earth. *J. Geophys. Res.* **90**, 2995–3007.

Condie, K. C. 1990. Growth and accretion of continental crust: inferences based on Laurentia. *Chem. Geol.* **83**, 183–194.

Ekart, D. D., Cerling, T. E., Montañez, I. P. and Tabor, N. J. 1999. A 400 million year carbon isotope record of pedogenic carbonate: implications for paleoatmospheric carbon dioxide. *Am. J. Sci.* **299**, 805–827.

Falkowski, P., Scholes, R. J., Boyle, E., Canadell, J., Canfield, D., Elser, J., Gruber, N., Hibbard, K., Högberg, P., Linder, S., Mackenzie, F. T., Moore III, B., Pedersen, T., Rosenthal, Y., Seitzinger, S., Smetacek, V. and Steffen, W. 2000. The global carbon cycle: A test of our knowledge of Earth as a system. *Science* **290**, 291–296.

Franck, S. 1998. Evolution of the global heat flow over 4.6 Gyr. *Tectonophysics* **291**, 9–18.

Franck, S. and Bounama, C. 1995. Effects of water-dependent creep rate on the volatile exchange between mantle and surface reservoirs. *Phys. Earth Planet. Inter.* **92**, 57–65.

Franck, S. and Bounama, C. 1997. Continental growth and volatile exchange during Earth's evolution. *Phys. Earth Planet. Inter.* **100**, 189–196.

Franck, S. and Bounama, C. 2001. Global water cycle and Earth's thermal evolution. *J. Geodyn.* **32**, 231–246.

Franck, S., Kossacki, K. J. and Bounama, C. 1999. Modelling the global carbon cycle for the past and future evolution of the earth system. *Chem. Geol.* **159**, 305–317.

Franck, S., Block, A., von Bloh, W., Bounama, C., Schellnhuber, H. J. and Svirezhev, Y. 2000a. Reduction of biosphere life span as a consequence of geodynamics. *Tellus* **52B**, 94–107.

Franck, S., von Bloh, W., Bounama, C., Steffen, M., Schönberner, D. and Schellnhuber, H.-J. 2000b. Determination of habitable zones in extrasolar planetary systems: Where are Gaia's sisters? *J. Geophys. Res.* **105**, E1,1651–1658.

Glaessner, M. F. and Foster, C. B. 1992. Paleontology and biogeochemical research: a powerful synergy. In: *Early organic evolution* (eds. M. Schidlowski, S. Golubic, M. M. Kimberley, D. M. McKirdy and P. A. Trudinger). Springer-Verlag, Berlin, 193–202.

Godderis, Y. and Veizer, J. 2000. Tectonic control of chemical and isotopic composition of ancient oceans: the impact of continental growth. *Am. J. Sci.* **300** ,434–461.

Grotzinger, J. P. and Kasting, J. F. 1993. New constrains on Precambrian ocean composition. *J. Geol.* **101**, 235–243.

Herzberg, C. T. 1995. Komatiite magmatism in the Archean mantle. In: *Abstract booklet (week A) of the XXI General Assembly of the IUGG,* Boulder, CO, 2–14 July 1995, 373.

Holland, H. D. 1978. *The chemistry of the atmosphere and oceans.* John Wiley, New York, 351 pp.

Holland, H. D. 1984. *The chemical evolution of the atmosphere and ocean.* Princeton University Press, Princeton, 582 pp.

Jambon, A. and Zimmermann, J. L. 1990. Water in oceanic basalts: Evidence for dehydration of recycled crust. *Earth Planet. Sci. Lett.* **101**, 323–331.

Junge, C. E., Schidlowski, M., Eichmann, R. and Pietrek, H. 1975. Model calculations for the terrestrial carbon cycle: Carbon isotope geochemistry and evolution of the photosynthetic oxygen. *J. Geophys. Res.* **80**, 4542–4552.

Kasting, J. F. 1984. Comments on the BLAG model: The carbonate-silicate geochemical cycle and its effect on atmospheric carbon dioxide over the past 100 million years. *Am. J. Sci.* **284**, 1175–1182.

Kasting, J. F. 1993. Earth's early biosphere. *Science* **259**, 920–926.

Kasting, J. F. and Ackermann, T. P. 1986. Climatic consequences of very high carbon dioxide levels in the Earth's early atmosphere. *Science* **234**, 1383–1385.

Kasting, J. F. and Walker, J. C. G. 1992. The geochemical cycle and the uptake of fossil fuel CO_2. In: *Global warming: Physics and facts* (eds. B. G. Levi, D. Hafemeister and R. Scribner). AIP Conference Proceedings 247, American Institute of Physics, New York, 175–200.

Kasting, J. F., Pavlov, A. A. and Siefert, J. L. 2001. A coupled ecosystem–climate model for predicting the methane

concentration in the Archean atmosphere. *Origins Life Evol. Biosphere* **31**, 271–285.

Kasting, J. F., Whitmire, D. P. and Reynolds, R. T. 1993. Habitable zones around main sequence stars. *Icarus* **101**, 108–128.

Kempe, S. and Degens, E. T. 1985. An early soda ocean? *Chem. Geol.* **53**, 95–108.

Kempe, S. and Kazmierczak, J. 1994. The role of alkalinity in the evolution of ocean chemistry, organization of living systems and biocalcification processes. *Bull. de l'Institut Océanographique, Monaco* **spécial 13**, 61–117.

Koster van Groos, A. F. 1988. Weathering, the carbon cycle and differentiation of the continental crust and mantle. *J. Geophys. Res.* **93**, 8952–8958.

Kump, L. R., Kasting, J. F. and Crane, R. G. 1999. *The Earth system*. Prentice Hall, Upper Saddle River, 351 pp.

Langmuir, C. H., Klein, E. M. and Plank, T. 1992. Petrological systematics of mid-ocean ridge-basalts: constraints on melt generation beneath ocean ridges. *Geophys. Monogr.* **71**, 183–280.

Lasaga, A. C., Berner, R. A. and Garrels, R. M. 1985. An improved geochemical model of atmospheric CO_2 fluctuations over the past 100 million years. In: *The carbon cycle and atmospheric CO_2: natural variations Archean to present* (eds. E. T. Sundquist and W. S. Broecker). Geophys. Monogr. Ser. 32, AGU, Washington, D.C., 397–411.

Lenton, T. M. 2000. Land and ocean carbon cycle feedback effects on global warming in a simple Earth system model. *Tellus* **52B**, 1159–1188.

Lenton, T. 2001. Introduction to the Gaia theory. In:, *Earth system science (Proceedings of the International School on Earth and Planetary Sciences, September 2000 at University of Siena, Italy)* (eds. S. Guerzoni, S. Harding, T. Lenton and F. Ricci-Lucchi). ISEPS, Siena, 9–29.

Lenton, T. M. and von Bloh, W. 2001. Biotic feedback extends the life span of the biosphere. *Geophys. Res. Lett.* **28**, 1715–1718.

Liu, L.-G. 1988. Water in the terrestrial planets and the moon. *Icarus* **74**, 98–107.

Macleod, G., McKeown, C., Hall, A. J. and Russell, M. J. 1994. Hydrothermal and ocean pH conditions of possible origin of life. *Origins Life Evol. Biosphere* **24**, 19–41.

McGovern, P. J. and Schubert, G. 1989. Thermal evolution of the Earth: effects of volatile exchange between atmosphere and interior. *Earth Planet. Sci. Lett.* **96**, 27–37.

McKenzie, D. and Bickle, M. J. 1988. The volume and composition of melt generated by extension of the lithosphere. *J. Petrol.* **29**, 625–679.

Ohmoto, H., Watanabe, Y., Yamaguchi, K. E., Ono, S., Bau, M., Kakegawa, T., Naraoka, H., Nedachi, M. and Lasaga, A. C. 2001. The Archaean atmosphere, oceans, continents and life. In: *Extended abstracts of the 4th International Archaean Symposium, 24-28 September 2001, Perth, Western Australia* (eds. K. F. Cassidy, J. M. Dunphy and M. J. Van Kranendonk). AGSO–Geoscience Australia, Record 2001/37, Australia,19–21.

Pavlov, A. A., Kasting, J. F., Brown, L. L., Rages, K. A. and Freedman, R. 2000. Greenhouse warming by CH_4 in the atmosphere of early Earth. *J. Geophys. Res.* **105**, 11981–11990.

Pearson, P. N. and Palmer, M. R. 2000. Atmospheric carbon dioxide concentrations over the past 60 million years. *Nature* **406**, 695–699.

Peixoto, J. P. and Oort, A. H. 1992. *Physics of climate*. Springer Verlag, New York, 520 pp.

Ringwood, A. E. 1975. *Composition and petrology of the Earth's mantle*. McGraw-Hill, New York, 618 pp.

Ronov, A. B. and Yaroshevsky, A. A. 1976. A new model for the chemical structure of the Earth's crust. *Geokhimiya* **12**, 1761–1795.

Ruddiman, W. 1998. Early uplift in Tibet? *Nature* **394**, 723–724.

Russell, M. J. and Hall, A. J. 1997. The emergence of life from iron monosulphide bubbles at a submarine hydrothermal redox and pH front. *J. Geol. Soc. Lond.* **154**, 377–402.

Rye, R., Kuo, P. H. and Holland, H. D. 1995. Atmospheric carbon dioxide concentrations before 2.2 billion years ago. *Nature* **378**, 603–605.

Sagan, C. and Chyba, C. 1997. The early faint young sun paradox: organic shielding of ultraviolet-labile greenhouse gases. *Science* **276**, 1217–1221.

Schidlowski, M. 1988. A 3800-billion-year isotopic record of life from carbon in sedimentary rocks. *Nature* **333**, 313–318.

Schubert, G. 1979. Subsolidus convection in the mantles of terrestrial planets. *Annu. Rev. Earth. Planet Sci.* **7**, 289–342.

Schwartzman, D. 1999. *Life, temperature and the Earth: the self-organizing biosphere*. Columbia University Press, New York, 241 pp.

Schwartzman, D. and Middendorf, G. 2000. Biospheric cooling and the emergence of intelligence. In: *A new era of bioastronomy* (eds. G. A. Lemarchand and K. J. Meech). ASP Conference Series, Vol. 213, 425–429.

Sleep, N.H. and Zahnle, K. 2001. Carbon dioxide cycling and implications for climate on ancient Earth. *J. Geophys. Res.* **106**, **E1**, 1373–1400.

Smyth, J. R. 1994. A crystallographic model for hydrous wadsleyite (β-Mg_2SiO_4): An ocean in the Earth's interior? *Am. Min.* **79**, 1021–1024.

Sprague, D. and Pollack, N. 1980. Heat flow in the Mesozoic and Cenozoic. *Nature* **285**, 393–395.

Stacy, F.D. 1992. *Physics of the earth*. Brookfield Press, Brisbane, Australia, 513 pp.

Staudacher, T. and Allègre, C. J. 1982. Terrestrial xenology. *Earth Planet. Sci. Lett.* **60**, 389–406.

Stumm, W. and Morgan, J. J. 1981. *Aquatic chemistry*. John Wiley, New York, 780 pp.

Svirezhev, Y. and von Bloh, W. 1998. A zero-dimensional climate-vegetation model containing global carbon and hydrological cycle. *Ecol. Modelling* **106**, 119–127.

Tajika, E. and Matsui, T. 1990. The evolution of the terrestrial environment. In: *Origin of the Earth* (eds. H. E. Newsom

and J. H. Jones). Oxford University Press, Oxford, 347–370.

Tajika, E. and Matsui, T. 1992. Evolution of terrestrial proto-CO_2 atmosphere coupled with thermal history of the Earth. *Earth Planet. Sci. Lett.* **113**, 251–266.

Turcotte, D. C. and Schubert, G. 1982. *Geodynamics*. John Wiley, New York, 450 pp.

Volk, T. 1987. Feedbacks between weathering and atmospheric CO_2 over the last 100 million years. *Am. J. Sci.* **287**, 763–779.

Walker, J. C. G. 1977. *Evolution of the atmosphere*,. Macmillan, New York, 318 pp.

Walker, J. C. G. 1985. Carbon dioxide on the early Earth. *Origins Life Evol. Biosphere* **16**, 117–127.

Walker, J. C. G., Hays, P. B. and Kasting, J. F. 1981. A negative feedback mechanism for the long-term stabilization of Earth's surface temperature. *J. Geophys. Res.* **86**, 9776–9782.

Walker, J. C. G., Klein, C., Schidlowski, M., Schopf, J. W., Stevenson, D. J. and Walter, M. R. 1983. Environmental evolution of the Archean-early Proterozoic Earth. In: *Earth's earliest biosphere: its origin and evolution* (ed. J. W. Schopf). Princeton University Press, Princeton, 260–290.

Wänke, H., Dreibus, G. and Jagouts E. 1984. Mantle chemistry and accretion history of the Earth. In: *Archean geochemistry* (eds. A. Kröaner et al.). Springer-Verlag, Berlin Heidelberg 1–24.

Wilde, S. A., Valley, J. W., Peck, W. H. and Graham, C. M. 2001. Evidence from detrial zircons for the existence of continental crust and oceans on the Earth 4.4 Gyr ago. *Nature* **409**, 175–178.